



Research article

Antileukemic activity of YPN-005, a CDK7 inhibitor, inducing apoptosis through c-MYC and FLT3 suppression in acute myeloid leukemia



Bon-Kwan Koo^a, Eun-Ji Choi^{a,*}, Eun-Hye Hur^{a,**}, Ju Hyun Moon^a, Ji Yun Kim^a, Han-Seung Park^a, Yunsuk Choi^a, Jung-Hee Lee^a, Kyoo-Hyung Lee^a, Eun Kyung Choi^b, Jinhwan Kim^c, Je-Hwan Lee^a

^a Department of Hematology, Asan Medical Center, University of Ulsan College of Medicine, Seoul, South Korea

^b Asan Preclinical Evaluation Center for Cancer Therapeutics, Asan Medical Center, Seoul, South Korea

^c R&D Institute, Yungjin Pharmaceutical Co., Ltd, South Korea

ARTICLE INFO

Keywords:

Acute myeloid leukemia (AML)
Cyclin dependent kinase 7 (CDK7) inhibitor
c-MYC
MCL1
FLT3

ABSTRACT

Acute myeloid leukemia (AML) is an aggressive blood cancer with a high rate of relapse associated with adverse survival outcomes, especially in elderly patients. An aberrant expression of cyclin dependent kinase 7 (CDK7) is associated with poor outcomes and CDK7 inhibition has showed antitumor activities in various cancers. We investigated the efficacy of YPN-005, a CDK7 inhibitor in AML cell lines, xenograft mouse model, and primary AML cells. YPN-005 effectively inhibited the proliferation of AML cells by inducing apoptosis and reducing phosphorylation of RNA polymerase II. The c-MYC expression decreased with treatment of YPN-005, and the effect of YPN-005 was negatively correlated with c-MYC expression. YPN-005 also showed antileukemic activities in primary AML cells, especially those harboring FMS-like tyrosine kinase 3–internal tandem duplication (FLT3-ITD) mutation and in *in vivo* mouse model. Phosphorylated FLT3/Signal transducer and activator of transcription 5 (STAT5) was decreased and FLT3/STAT5 was downregulated with YPN-005 treatment. Our data suggest that YPN-005 has a role in treating AML by suppressing c-MYC and FLT3.

1. Introduction

Acute myeloid leukemia (AML) is an aggressive myeloid neoplasm with the highest incidence in the elderly with a median age of diagnosis at 68 years. Although high-intensity treatments including intensive induction chemotherapy followed by allogeneic stem cell transplantation offer long-term survival in some percentage of young and fit patients, substantial number of patient experience disease relapse. In addition, the treatment outcomes are even worse in older patients because of unfavorable genetic features, antecedent hematologic diseases, and poor performance status. Some targeted agents, IDH inhibitors, FLT3 inhibitors, and BCL-2 inhibitor showed improved response rates in patients who relapsed, are refractory or unfit old AML patients. However, the duration of response rate and long-term outcomes remained unsatisfactory (Almeida and Ramos, 2016; Medeiros et al., 2015).

Cyclin dependent kinases (CDKs) play a crucial role in controlling cell cycle progression and transcription regulation. Certain CDKs are

involved in cell cycle regulation, whereas several other CDKs in control gene transcription by phosphorylating RNA polymerase II (Malumbres, 2014). CDK7, a CDK family member, has an important function in transcription regulation and cell cycle transition (Diab et al., 2020). It controls gene transcription through phosphorylation at serine 5 and 7 of RNA polymerase II required for transcription initiation (Glover-Cutter et al., 2009; Mosley et al., 2009). Previously reported aberrant expression of CDK7 in various solid tumors has been correlated with poor clinical outcomes and aggressive pathological parameters (J. R. Huang et al., 2018; Wang et al., 2018; Zhou et al., 2019). Therefore, CDK7 has been considered as a potential target for cancer treatment, and its inhibition has been shown to have antitumor effects by suppressing cell proliferation and impeding cell cycle progression in various cancer cells (Diab et al., 2020). CDK7 blockade has been associated with transcriptional repression of proto-oncogenes such as c-MYC gene family and tumor regression in solid cancer (Chipumuro et al., 2014; Christensen et al., 2014).

* Corresponding author.

** Corresponding author.

E-mail addresses: eunjicho@amc.seoul.kr (E.-J. Choi), gracehur@amc.seoul.kr (E.-H. Hur).

Several CDK7 inhibitors have showed antileukemic effects in pre-clinical AML models. CT7001 and SY-1365, inhibitors of CDK7, have shown to inhibit cell proliferation both in AML cell lines and tumor growth in a xenograft model. Their antileukemic effects were attributed to induction of apoptotic cell death and decreased expression of c-MYC and MCL1 (Clark et al., 2017; Hu et al., 2019). c-MYC has been shown to be frequently activated in AML and plays an important role in the induction of leukemogenesis and leukemic progression (Liman et al., 2020; Luo et al., 2005). Moreover, c-MYC overexpression contributes to leukemia stem cell self-renewal, cell growth, and drug resistance in AML cells (Pan et al., 2014). However, the efficacy and mechanism of CDK7 inhibitors in AML remain to be elucidated further.

YPN-005, a highly selective CDK7 inhibitor, showed antiproliferative effects in primary sample and drug-resistant lung cancer (Choi et al., 2021). Therefore, in this study, we explored the potential efficacy of YPN-005 in AML cell lines, mouse models, and primary cells from AML patients. In addition, we also evaluated a possible mechanism of the antileukemic effect of YPN-005 in AML.

2. Material and methods

2.1. Cell lines and compounds

The information on cell lines has been described in Supplementary T 1. YPN-005 (C₂₆H₂₈N₆O₂S) and SY1365 were kindly provided from Yungjin Pharm. Co., Ltd (Gyeonggi-do, Korea) (Choi et al., 2021), venetoclax (cat. no. S8048) and gilteritinib (cat. no. S7754) were purchased from Selleck Chemicals (Houston, TX), and cytarabine (cat. no. SC1768), azacitidine (cat. no. A2385), and decitabine (cat. no. A3656) were purchased from Sigma-Aldrich (St. Louis, MO).

2.2. Patient sample

Primary mononuclear cells were collected from bone marrow (BM) samples of 26 AML patients enrolled in this study (Supplementary T 2). Informed consents were obtained from the patients in accordance with Declaration of Helsinki, and the protocol was approved by the institutional review board of Asan Medical Center (2016-1373). All samples were stored in Bio-Resource Center in Asan Medical Center (Seoul, Korea).

2.3. Ex vivo assay

Cryopreserved BM cells were washed with ice-cold phosphate-buffered saline and then counted using acridine orange (AO)/propidium iodide (PI) (Nexcelom, Lawrence, MA) staining method. For cell viability assay, 2×10^4 cells/well were seeded in a 96-well opaque plate (SPL Life Science, Korea) in complete media and incubated with 20 nM and 100 nM of YPN-005 for 3 days in a humidified atmosphere with 5% CO₂ at 37 °C. The complete media was composed of X-Vivo™ 15 media (Lonza, Switzerland), supplemented with 20% fetal bovine serum (Hyclone Inc., Logan, UT), 50 ng/mL IL-3 (R&D systems, Inc., Minneapolis, MN), 40 ng/mL IL-6 (R&D systems, Inc.), 200 ng/mL GM-CSF (R&D systems, Inc.), 200 ng/mL G-CSF (R&D systems, Inc.), 2 mM L-glutamine (Thermo Fisher Scientific, UK), 4 U/mL EPO (R&D systems, Inc.), and 5.5¹⁰⁻⁵ β-mercaptoethanol (Sigma-Aldrich). Cell proliferation was evaluated using CellTiter-Glo® Luminescent Cell Viability Assay (Promega Corp., Madison, WI) following manufacturer's protocol. Luminescence was detected using Victor3 multilabel plate reader following manufacturer's protocol (PerkinElmer, Waltham, MA).

2.4. Reverse transcription quantitative polymerase chain reaction

Isolated total RNA following manufacturer's protocol (RNeasy® Plus Mini Kit, Qiagen GmbH, Germany) was converted to cDNA using RevertAid First Strand cDNA Synthesis Kit (Thermo Fisher Scientific), according to the manufacturer's recommendation. Quantitative PCR was

performed using LightCycler® 480 SYBR Green Master mix (Roche, Switzerland) for *FLT3*, *STAT5*, *c-MYC*, *MCL1*, *β-actin*, and *18s* with specific primers listed in Supplementary T 3. Relative fold changes in mRNA expression were calculated using formula $2^{-\Delta\Delta CT}$.

2.5. Measurement of apoptosis

Here 1×10^6 cells were seeded in 6-well plates and incubated with different concentrations of YPN-005 for 24 h. Thereafter, the cells were harvested and stained with Annexin V-FITC apoptosis detection kit I (BD Biosciences, Franklin Lakes, NJ) following the manufacturer's protocol. Stained cells were measured via flow cytometry on FACSCanto II (BD Bioscience) and analyzed using BD FACSDiva v8.0.2 software (BD Bioscience).

2.6. Immunoblotting

Cell lysates were prepared using cell lysis buffer (Cell Signaling Technology, Inc., Danvers, MA). Then, incubated with Xpert protease inhibitor cocktail solution (GenDEPOT, Barker, TX) and phosphatase inhibitor cocktail set II (Calbiochem, EMD Biosciences, Inc. La Jolla, CA) on ice for 30 min and centrifuged at $14,000 \times g$ for 10 min at 4 °C. The protein concentration was measured using Bradford (Coomassie) protein assay plus kit (GenDEPOT) and 595 nm absorption was measured using molecular devices SpectraMax M2 Multilabel Microplate Reader (Marshall Scientific, Hampton, NH). A total of 10 μg protein extract was loaded onto a SDS polyacrylamide gel. Following electrophoresis, proteins were transferred to polyvinylidene difluoride membranes (Bio-Rad Laboratories, Inc. Hercules, CA) and had blocked with 2% skim milk for 30 min and then the primary antibodies listed in Supplementary T 4 at a dilution of 1:1,000 at 4 °C overnight. The blots were incubated with a secondary horseradish peroxidase (HRP)-conjugated specific antibody (Enzo Life sciences, Inc. Farmingdale, NY) 1:3,000 at room temperature for 1 h. The signal was visualized using an enhanced BioFX chemiluminescent sensitive plus HRP microwell and/or membrane substrate (BioRX Laboratories, Owning Mills, MD), and chemiluminescence was measured using Ez-capture ST system (ATTO Corporation, Japan). Quantification of Immunoblot band intensity was performed using CS analyzer 4 software (ATTO Corporation).

2.7. In vivo orthotopic mouse model

Lentiviral products was harvested using pCDH-CMV-MCS-EF1a-GFP (Addgene, CD513B-1, Cambridge, MA) as expressing vector, pMDLg/pRRE and pRSV-REV as packaging plasmid, and pH27G as envelope plasmid in 293FT cell line. The lentiviral particles was infected into MOLM-13 cell line using 8 μg/mL polybrene (TR-1003, Sigma-Aldrich) and then selected using 5 μg/mL puromycin (Enzo Life sciences, Inc. Farmingdale, NY). Animal experiments were conducted in accordance with the guidelines of the Institutional Animal Care and Use Committee of the Asan Medical Center (2020-12-080). Leukemic orthotopic mouse model was established by tail-vein injection of 5×10^6 pGFP-transduced MOLM-13 cells in 6 weeks female NSG mouse (Jackson Laboratory, Bar Harbor, ME). YPN-005 at a dose of 1 or 2 mg/kg was injected intravenously via tail vein on 2-day-on/5-day-off or a biweekly schedule. Tumor load was measured based on bioluminescence imaging using the IVIS spectrum *in vivo* imaging system (PerkinElmer) after epilation. Fluorescence signal intensity was quantified using the Living Imaging software (PerkinElmer).

2.8. Statistical analysis

Data analysis for cell viability, apoptosis, and mRNA expression was performed using one-way analysis of variance followed by *post hoc* Tukey's multiple comparisons or Bonferroni tests when appropriate. To evaluate the correlation between cell viability and *FLT3*-ITD mutation in

patient samples, we used Student's t-test or Mann–Whitney U test as appropriate. A relationship between cell viability and protein expression was evaluated using Spearman's correlation. The Survival analyses were performed using the Kaplan–Meier method and the resulting survival curves were compared using the log-rank test. The graphs were plotted and analyzed using GraphPad Prism 5 (GraphPad Software, Inc. La Jolla) and $p < 0.05$ was considered to indicate a statistical significance. Data were accumulated from three independent experiments and presented as mean \pm standard deviation (SD).

3. Results

3.1. YPN-005 effectively inhibits proliferation of various AML cell lines

To evaluate the efficacy of YPN-005 in AML, we screened the cell growth inhibitory activity of YPN-005 in nine AML cell lines (Table 1 and Supplementary F 1). It was observed that upon comparison with SY1365 (a CDK7 inhibitor) and other anti-leukemic medications including daunorubicin, cytarabine, and venetoclax, YPN-005 showed similar or superior efficacy. Venetoclax was observed to be highly sensitive in cell lines MOLM-13, MOLM-14, MV4-11, and OCI-AML2. However, cytarabine and daunorubicin, a backbone of cytotoxic chemotherapy in AML, showed heterogeneous results. YPN-005, however, showed a similar antiproliferative activities at IC₅₀ concentrations ranging from 1.95 to 29.04 nM in all cell lines, suggesting that it might have an antileukemic efficacy irrespective of specific biologic characteristics of each AML cell lines.

3.2. YPN-005 induces apoptosis in AML cell lines in a dose-dependent manner

To identify the mechanism by which YPN-005 exhibits growth inhibitory effects in AML cells, we performed FACS analysis using Annexin V/PI staining and immunoblotting assay 24 h post treatment with YPN-005 in AML cell lines. Apoptosis was observed in all three AML cell lines (MOLM-13, OCI-AML2, and U937), and it increased with increasing dose of YPN-005 as shown in Figure 1A, B. In concordance with flow cytometric results, immunoblotting revealed an increase in cleaved poly (ADP-ribose) polymerase (PARP) and caspase-3, and a decrease in X-linked inhibitor of apoptosis protein (XIAP) in YPN-005-treated AML cell lines, which indicate induction of apoptosis (Figure 1C). Together, the above results suggest that YPN-005 induces apoptosis in AML cells in a dose-dependent manner.

3.3. YPN-005 suppresses CDK7-dependent RNA polymerase phosphorylation and c-MYC expression

It has been reported previously that CDK7 indirectly regulates transcription of MCL1 (Tibes and Bogenberger, 2019), and the expression of c-MYC and MCL1 is reduced by the CDK7 inhibitor (T. Huang et al., 2019; Li et al., 2017). In addition, c-MYC seems to directly control the transcription of MCL1 in gastric cancer cells (Labisso et al., 2012). Thus, to evaluate the mechanism of YPN-005 in AML cell lines, the protein expression of MCL1, c-MYC, and phosphorylated RNA polymerase (Rpb)

was determined using immunoblot assay (Figure 2A). It was observed that the expression of MCL1, c-MYC, and phosphorylated Rpb decreased with YPN-005 treatment. Moreover, the mRNA expression of c-MYC was observed to be suppressed with increasing dose of YPN-005 in all three cell lines, whereas that of MCL1 was decreased in OCI-AML2 cell line but not in MOLM-13 and U937 showing inconsistent results between cell lines (Figure 2B). These results suggest that YPN-005 induced an antileukemic effect by controlling the transcriptional regulation of c-MYC.

We further examined the endogenous c-MYC and MCL1 protein expression levels in AML cell lines and its correlation with drug sensitivities (Supplementary F 2). As shown in Figure 2C, positive correlation was observed between the IC₅₀ value of YPN-005 and c-MYC expression with correlation coefficient of 0.762 ($p = 0.017$), whereas no such significant correlation could be observed with MCL1 expression (correlation coefficient = 0.650, $p = 0.158$).

We also assessed the cell cycle status in MOLM-13 and MOLM-14 cell lines upon treatment with different concentrations of YPN-005, but no significant change in accumulation pattern was observed compared to baseline (Supplementary F 3). Taken together, these results indicate that the antileukemic activity of YPN-005 in AML cells is possibly derived from transcription regulation through RNA polymerase II with c-MYC regulation rather than cell cycle arrest to induce apoptosis.

3.4. YPN-005 shows antileukemic efficacy in in vivo and ex vivo preclinical models

Thereafter, we evaluated the efficacy of YPN-005 in an orthotopic mouse model generated using GFP-transduced MOLM-13 cell line. The tumor load was assessed using fluorescent imaging. YPN-005-treated groups showed significantly improved survival compared with control group ($p < 0.01$) (Figure 3A). The median survival of each group was as follows: 18 days in control group, 24 days in 1 mg/kg group, 35 days in 2 mg/kg of 2 days-on/5 days-off group, and 42 days in 2 mg/kg biweekly (BIW) group, respectively. Rapid and prominent weight loss was observed in the control group compared to the YPN-005 treated groups (Figure 3B). Fluorescent imaging showed that YPN-005 treatment induced suppression of luminescence (Figure 3C) indicating a cytostatic rather than cytotoxic activity of YPN-005 against AML cells. In one of the 2 mg/kg BIW-treated groups, a lump was observed on flank at 31 days, which not only increased in size, but also spread to the groin by 38 days despite the decrease in body volume (Supplementary F 4).

Further to delineate the efficacy of YPN-005, a cell proliferation inhibition assay in primary leukemic cells obtained from 26 AML patients was performed (Supplementary F 5). YPN-005 showed significant growth inhibition in primary AML cells in a dose-dependent manner (Figure 3D). AML cells harboring FLT3-ITD mutation ($n = 18$) were found to be significantly more sensitive to YPN-005 compared with cells without this mutation ($n = 8$) (Figure 3E and F).

3.5. YPN-005 suppresses the FLT3-STAT5 pathway

YPN-005 exhibited potential antileukemic properties in AML cells with FLT3-ITD mutation; therefore, we examined the changes in mRNA and protein expression levels of FLT3 and STAT5, a known downstream

Table 1. IC₅₀ values of three approved leukemic drugs (daunorubicin, cytarabine, and venetoclax) and two CDK7 inhibitors (YPN-005 and SY1365) measured in AML cell lines. The cell viability was assessed using CellTiter-Glo® assay after 72 h.

	IC ₅₀ value (nM)								
	MOLM-13	MOLM-14	MV4-11	OCI-AML2	THP-1	U937	KG-1	SKM-1	BDCM
YPN-005	18.99	2.77	11.82	7.74	1.95	2.43	29.04	25.04	2.68
SY1365	10.68	2.33	16.95	15.6	5.92	6.54	70.88	26.76	14.53
Daunorubicin	7.76	14.53	3.63	7.92	24.85	5.68	231.3	12.56	7.2
Cytarabine	89.34	274.2	555.5	233.6	192.5	59.76	544.6	>1,000	>1,000
Venetoclax	396.4	0.41	172.6	14.7	>1,000	>1,000	>1,000	>1,000	>1,000

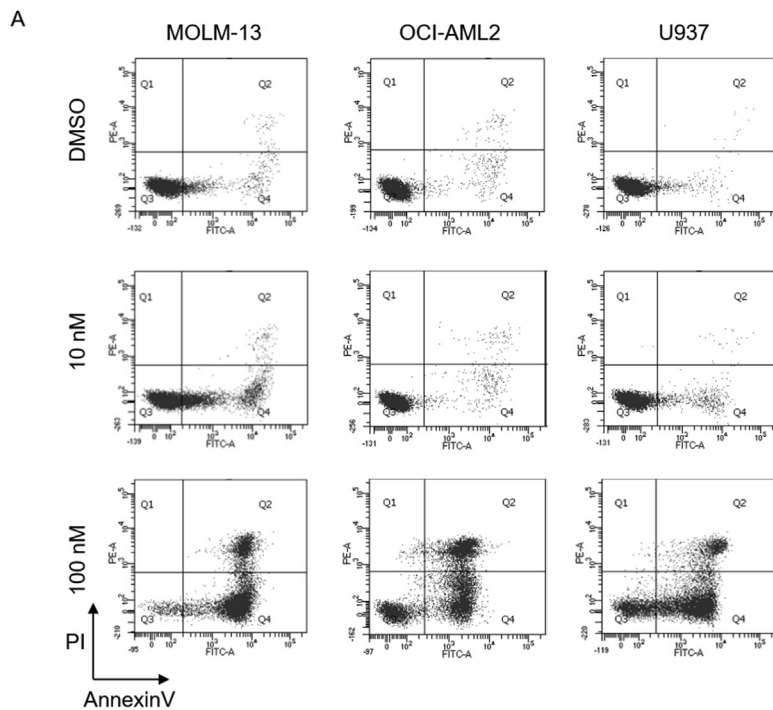
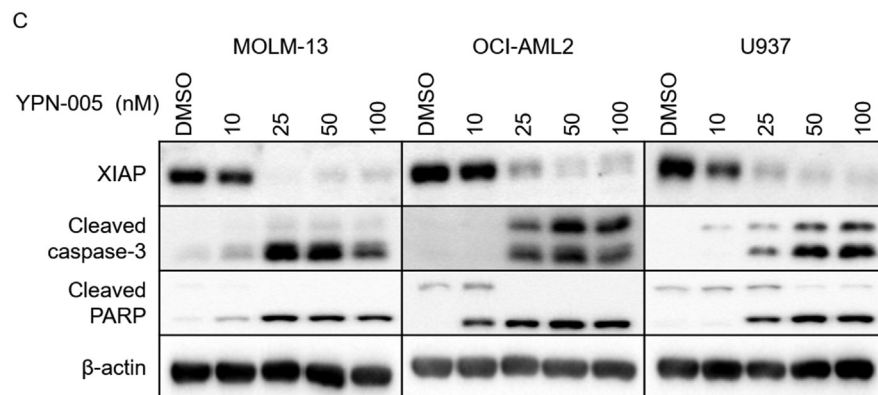
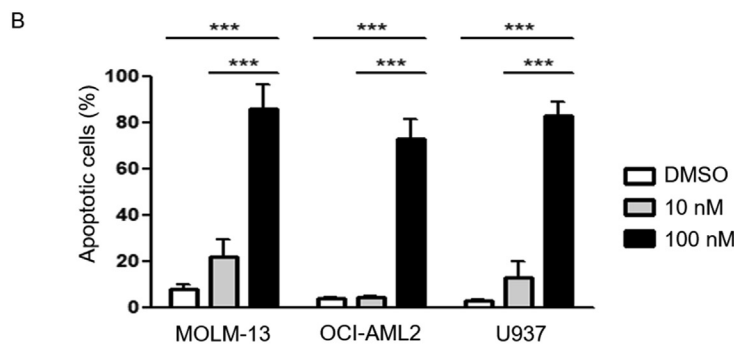


Figure 1. Apoptotic effect of YPN-005 in MOLM-13, OCI-AML2, and U937 cell lines. Apoptosis was evaluated using Annexin V/PI staining (A, and B) and immunoblot assay (C) of 0, 10 and 100 nM YPN-005 treated cell lines. Scatter plot (A) and apoptosis percentage (B) measured after incubation with YPN-005 for 24 h * $p < 0.05$, ** $p < 0.01$ and *** $p < 0.001$ was considered to be statistically significant. (C) expression of cleaved PARP and caspase 3 cleavage, and XIAP was determined using immunoblot assay of after 24 h of 0, 10, 25, 50, and 100 nM YPN-005 exposure. 0.001% Dimethyl sulfoxide (DMSO) was used as a negative or positive control.



signaling molecules for FLT3. It was observed that both the RNA expression of *FLT3* and *STAT5* and phosphorylated protein expression of FLT3 and *STAT5* decreased post treatment with YPN-005 in a dose-dependent manner in all three cell lines as shown in Figure 4a and b.

Even though OCI-AML2 cells do not harbor *FLT3* gene mutation, the overexpressed levels of endogenous phosphorylated form of FLT3 decreased after YPN-005 treatment. Moreover, in order to confirm the expression status of FLT3 in OCI-AML2 cells, they were treated with

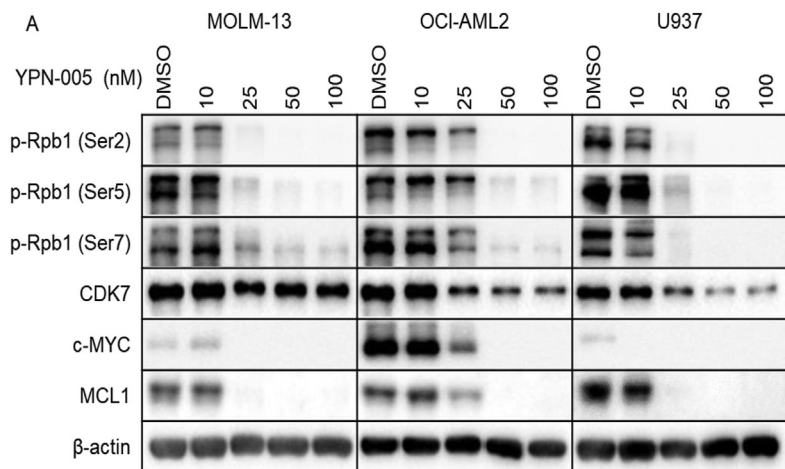
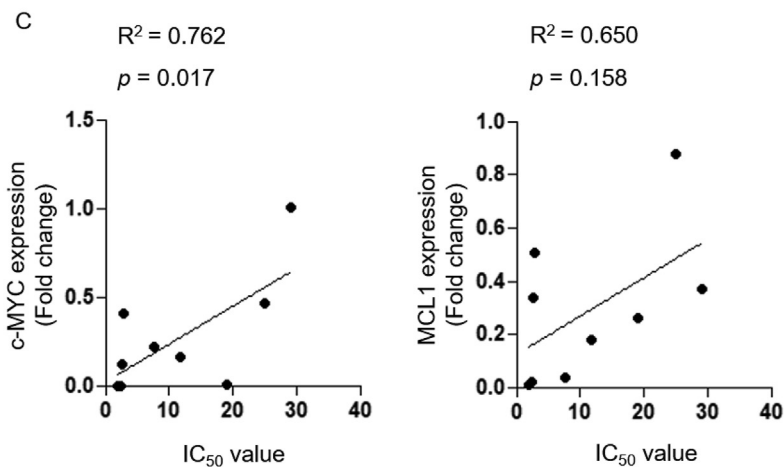
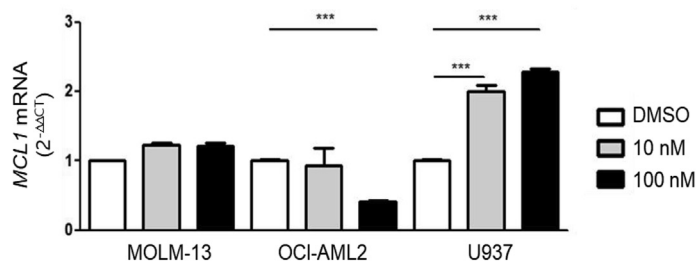
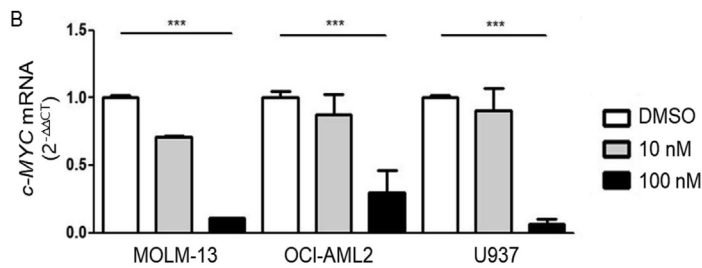


Figure 2. Regulation of c-MYC by YPN-005 in MOLM-13, OCI-AML2, and U937 cell lines. (A) Protein expression measured for RNA polymerase II protein (p-Rpb1 [Ser2, 5, and 7]), CDK7, c-MYC, MCL1 in a dose-dependent manner post treatment with YPN-005 after 24 h β-actin was used as a loading control. (B) mRNA expression measured post treatment with YPN-005 after 24 h. (C) Correlation between IC₅₀ value of YPN-005 and protein expression of c-MYC and MCL1 in AML cell lines. **p* < 0.05, ***p* < 0.01 and ****p* < 0.001 was considered to be statistically significant.



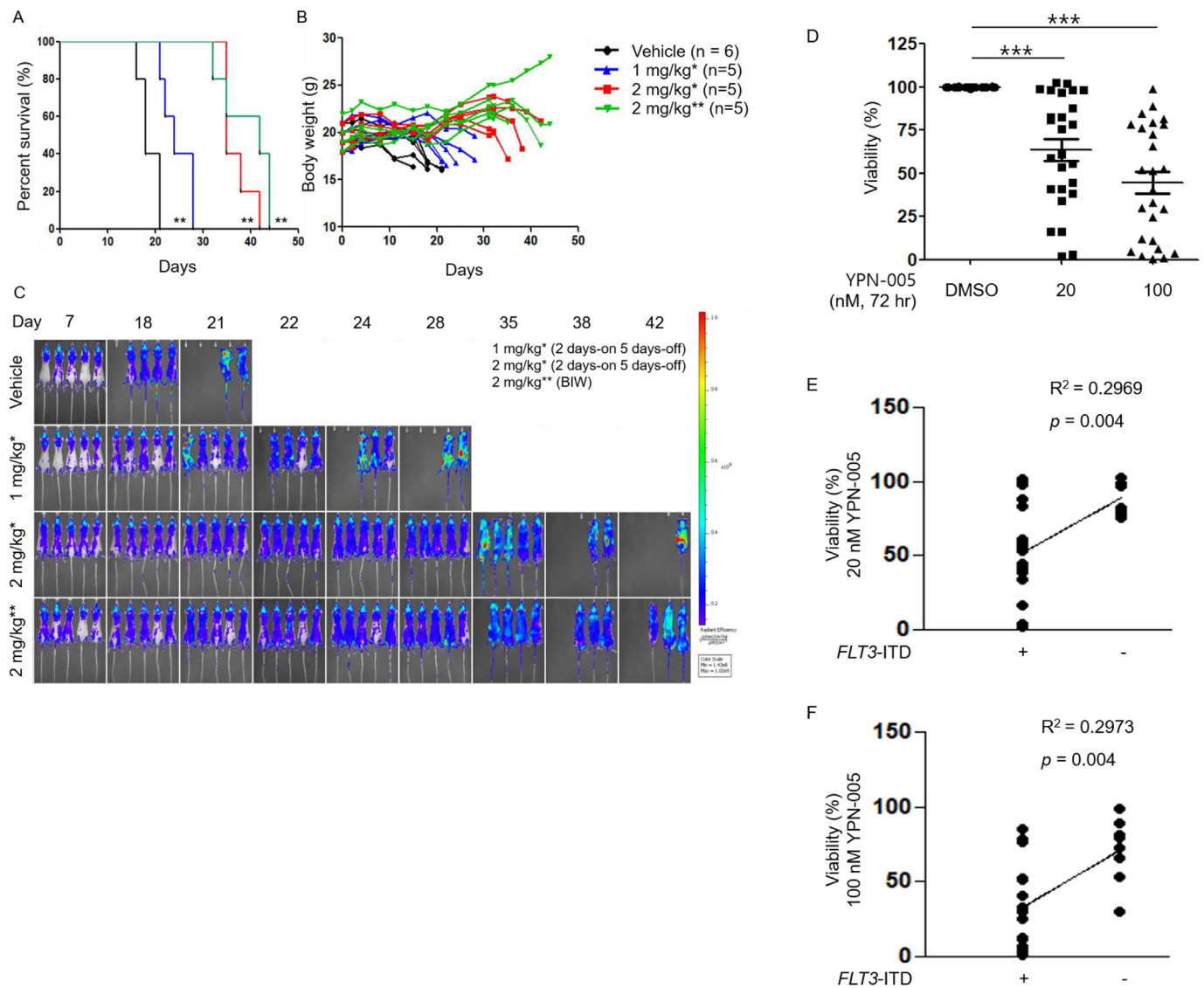


Figure 3. Antileukemic effect of YPN-005 in *in vivo* (A–C) and *ex vivo* (D–F) AML models. (A) Kaplan–Meier survival curve and (B) Change of whole mice body weight. (C) Assessment of the IVIS imaging in the orthotopic xenograft mouse model using GFP-transduced MOLM-13 cell line. YPN-005 was administered intravenously with a dose of 1 or 2 mg/kg initiated 2 days after injection with leukemia cells. The treatment was scheduled as follows: 1) *2-day-on/5-day-off and 2) **biweekly (BIW), $\times 3$ cycles. (d) Primary human AML cells were treated with indicated YPN-005 concentrations for 72 h, and cell viability was assessed using CellTiter-Glo[®] assay. The linear correlation between *FLT3*-ITD mutation status (+vs. –) and viability percentage at 20 nM (e) and 100 nM (f) concentration of YPN-005 was measured. For survival, $**p < 0.01$ was considered to be statistically significant.

gilteritinib. The viability assay showed that antiproliferative effect of gilteritinib in OCI-AML2 cells was higher than that in U937 cell line (Supplementary F 6), suggesting that YPN-005 shows antileukemic effects by suppressing *FLT3* and *STAT5* irrespective of *FLT3* mutation status.

4. Discussion

In this study, YPN-005, a CDK7 inhibitor, exerted potent antileukemic activity in AML both *in vitro* and *in vivo* by inducing apoptotic cell death. These apoptosis-inducing antiproliferative effects of YPN-005 were related to inhibition of c-MYC and MCL1 expression consistent with previous reports. Several CDK7 inhibitors have showed anticancer effects by inducing cell apoptosis in AML, B-cell acute lymphoblastic leukemia, and solid tumors (Abudurehman et al., 2021; Clark et al., 2017; Hu et al., 2019; T. Huang et al., 2019; Li et al., 2017; Zhang et al., 2019; Zhong et al., 2019). In addition, inhibition of CDK7 has been associated with decreased expression of c-MYC and MCL1 (Clark et al., 2017; Li

et al., 2017). Association between CDK7 inhibition and repression of MYC-driven transcriptional core set has been well described in MYC-driven medulloblastoma models (Veo et al., 2021). A previous study showed that THZ1 treatment induced downregulation of genes, which have a significant association with DNA repair function by diminishing RNA polymerase II and MYC association. We observed that both protein and mRNA levels of c-MYC were downregulated with YPN-005 treatment, but only protein expression was consistently suppressed for MCL1. Similar finding was also reported in a previous study of SY-1365, a CDK7 inhibitor where SY-1365 treatment was associated with decreased protein expression of MCL1 but not its mRNA expression (Hu et al., 2019). Although CDK inhibitors are known to target MCL1 indirectly, the exact mechanism of regulating MCL1 expression through blocking CDK7 is not well identified. As MCL1 is regulated by numerous modulators at multiple cellular levels including transcription, translation, ubiquitination, and degradation, further research is warranted to reveal the mechanism of MCL1 downregulation using CDK7 inhibitors (Senichkin et al., 2020).

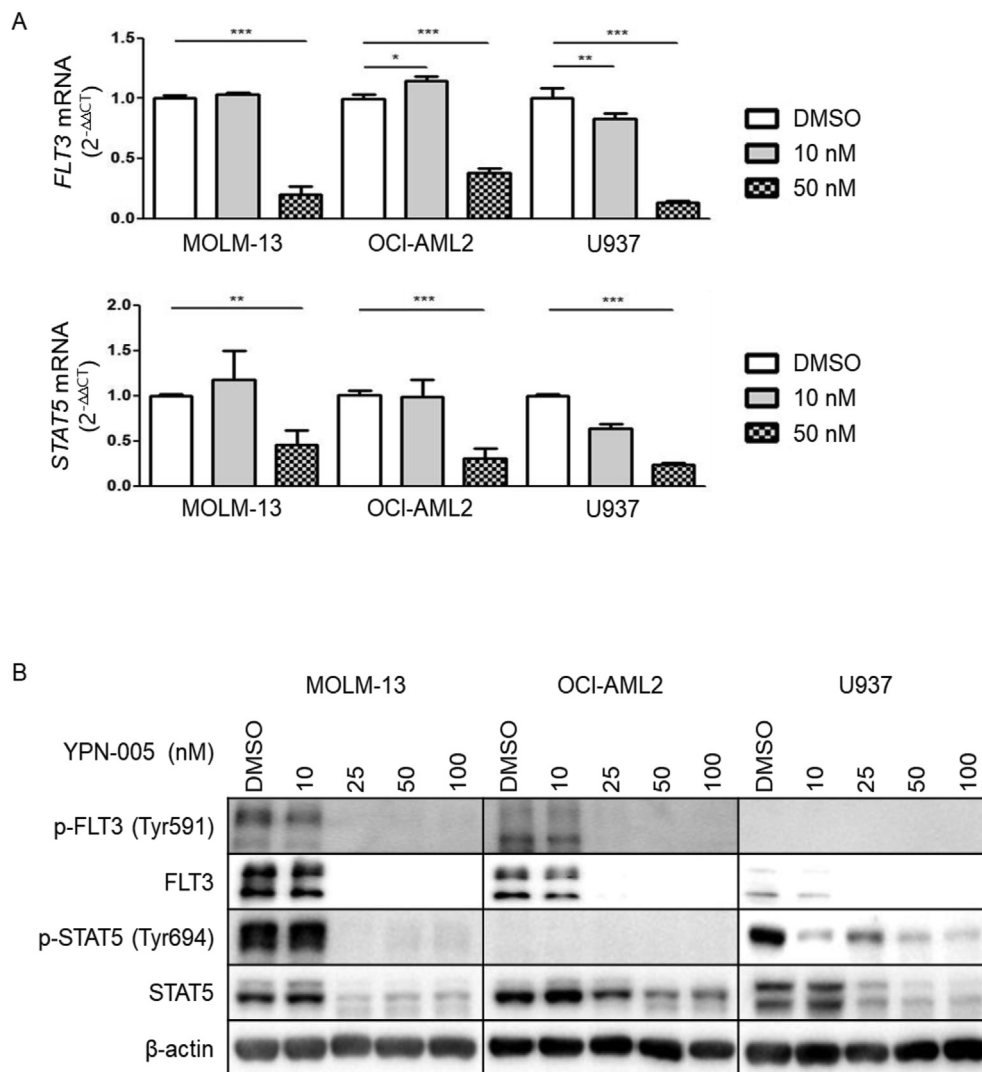


Figure 4. Regulation of FLT3 signaling pathway by YPN-005 in MOLM-13, OCI-AML2, and U937 cell lines. All cell lines were treated with increasing concentration of YPN-005 for 24 h FLT3 and STAT5 mRNA (A) and protein (B) expression following YPN-005 treatment was measured.

Another known function of CDK7 is regulating cell cycle by forming CDK-activating kinase, which leads to the phosphorylation of CDK4/6 (Diab et al., 2020). Previous studies have shown that when CDK7 was selectively inhibited in colon cancer cells, both CDK1 and CDK2 were activated and cell-cycle arrest was induced at G1/S and G2/M phase, respectively (Larochelle et al., 2007).

We also observed that YPN-005 effectively inhibited proliferation of FLT3-ITD mutated primary AML cells and downregulated FLT3 and STAT5 expression in both FLT3-ITD mutated or FLT3 unmutated AML cell lines. To the best of our knowledge, this is the first finding to show the potential inhibitory property of CDK7 inhibition on FLT3 downstream signaling. A previous study demonstrated that a small molecule inhibitor that co-targets CK1 α and CDK7/9 showed antileukemic activity in FLT3-ITD mutated mouse models where inhibition of both CK1 α and CDK7/9 was related to stabilization of p53 leading to apoptosis of leukemia cells, but the effect on FLT3-STAT5 pathway was not fully discovered (Minzel et al., 2018). Our finding suggested that CDK7 blockade could be one of the therapeutic strategies for FLT3-mutated AML and further mechanistic evidence needs to be gathered.

In clinical setting, there have been phase I or II clinical trials with several CDK7 inhibitors including SY1365 (clinical trial number NCT03134638), SY-5609 (clinical trial number NCT04247126), CT7001 (clinical trial number NCT03363893), and LY3405105 (clinical trial

number NCT03770494) in patients with advanced solid tumors. Some trials were terminated because of lack of efficacy or presence of toxicities, which is expected because CDK7 is ubiquitously expressed in all cell types. Our *in vivo* study showed that YPN-005 treatment prolonged survival of orthotopic xenograft mouse models with no significant weight loss or phenotypical injuries. In this regard, YPN-005 might be of an effective and feasible therapeutic value in AML, and should be studied further.

However, our study had certain limitations. First, while CDK7 is well known to be involved in the transcription cycle of RNA polymerase II and the inhibitory effects of YPN-005 were observed in this study, the genetic studies regarding the relevant targets of YPN-005 were not fully addressed. Second, the mechanistic studies regarding CDK7 inhibition and decreased expression of c-MYC and MCL1 are lacking. Despite these limitations, our study provided some evidences of efficacy and novel mechanism of a CDK7 inhibitor in AML.

In conclusion, our results demonstrate that YPN-005, a CDK7 inhibitor showed a significant antiproliferative efficacy in AML both *in vitro* and *in vivo* by inducing apoptosis. Moreover, YPN-005 treatment suppressed the expression of c-MYC and FLT3-STAT5. Therefore, this study provides substantial preclinical evidence of YPN-005 being a potential candidate for future therapeutic strategies to treat AML patients.

Declarations

Author contribution statement

Bon-Kwan Koo: Conceived and designed the experiments; Performed the experiments; Wrote the paper.

Eun-ji Choi: Conceived and designed the experiments; Contributed reagents, materials, analysis tools or data; Wrote the paper.

Eun-Hye Hur: Conceived and designed the experiments; Wrote the paper.

Ju Hyun Moon; Ji Yun Kim: Performed the experiments.

Han-Seung Park; Yunsuk Choi; Kyoo-Hyung Lee; Eun Kyung Choi; Jinhwan Kim; Je-Hwan Lee: Contributed reagents, materials, analysis tools or data.

Jung-Hee Lee: Analyzed and interpreted the data.

Funding statement

Eun Kyung Choi was supported by the Ministry of Health & Welfare, Republic of Korea [HI20C1586].

Data availability statement

Data included in article/supp. material/referenced in article.

Competing interest statement

The authors declare no conflict of interest.

Additional information

Supplementary content related to this article has been published online at <https://doi.org/10.1016/j.heliyon.2022.e11004>.

Acknowledgements

We would like to thank Editage (www.editage.co.kr) for English language editing.

References

- Abudurehman, T., Xia, J., Li, M.H., Zhou, H., Zheng, W.W., Zhou, N., Shi, R.Y., Zhu, J.M., Yang, L.T., Chen, L., Zheng, L., Xue, K., Qing, K., Duan, C.W., 2021. CDK7 inhibitor THZ1 induces the cell apoptosis of B-cell acute lymphocytic leukemia by perturbing cellular metabolism. *Front. Oncol.* 11, 663360.
- Almeida, A.M., Ramos, F., 2016. Acute myeloid leukemia in the older adults. *Leuk. Res. Rep.* 6, 1–7.
- Chipumuro, E., Marco, E., Christensen, C.L., Kwiatkowski, N., Zhang, T., Hatheway, C.M., Abraham, B.J., Sharma, B., Yeung, C., Altabef, A., Perez-Atayde, A., Wong, K.K., Yuan, G.C., Gray, N.S., Young, R.A., George, R.E., 2014. CDK7 inhibition suppresses super-enhancer-linked oncogenic transcription in MYCN-driven cancer. *Cell* 159, 1126–1139.
- Choi, Y.J., Lee, H., Kim, D.S., Kim, D.H., Kang, M.H., Cho, Y.H., Choi, C.M., Yoo, J., Lee, K.O., Choi, E.K., Lee, J.C., Rho, J.K., 2021. Discovery of a novel CDK7 inhibitor YPN-005 in small cell lung cancer. *Eur. J. Pharmacol.* 907, 174298.
- Christensen, C.L., Kwiatkowski, N., Abraham, B.J., Carretero, J., Al-Shahrour, F., Zhang, T., Chipumuro, E., Herter-Sprie, G.S., Akbay, E.A., Altabef, A., Zhang, J., Shimamura, T., Capelletti, M., Reibel, J.B., Cavanaugh, J.D., Gao, P., Liu, Y., Michaelsen, S.R., Poulsen, H.S., Aref, A.R., Barbie, D.A., Bradner, J.E., George, R.E., Gray, N.S., Young, R.A., Wong, K.K., 2014. Targeting transcriptional addictions in small cell lung cancer with a covalent CDK7 inhibitor. *Cancer Cell* 26, 909–922.
- Clark, K., Ainscow, E., Peall, A., Thomson, S., Leishman, A., Elaine, S., Ali, S., Coombes, R., Barrett, A., Bahl, A.K., 2017. CI7001, a novel orally bio-available CDK7 inhibitor, is highly active in in-vitro and in-vivo models of AML. *Blood* 130 (Suppl 1), 2645.

- Diab, S., Yu, M., Wang, S., 2020. CDK7 inhibitors in cancer therapy: the sweet smell of success? *J. Med. Chem.* 63, 7458–7474.
- Glover-Cutter, K., Larochelle, S., Erickson, B., Zhang, C., Shokat, K., Fisher, R.P., Bentley, D.L., 2009. TFIIH-associated Cdk7 kinase functions in phosphorylation of C-terminal domain Ser7 residues, promoter-proximal pausing, and termination by RNA polymerase II. *Mol. Cell Biol.* 29, 5455–5464.
- Hu, S., Marineau, J.J., Rajagopal, N., Hamman, K.B., Choi, Y.J., Schmidt, D.R., Ke, N., Johannessen, L., Bradley, M.J., Orlando, D.A., Alnemy, S.R., Ren, Y., Ciblat, S., Winter, D.K., Kabro, A., Sprott, K.T., Hodgson, J.G., Fritz, C.C., Carulli, J.P., di Tomaso, E., Olson, E.R., 2019. Discovery and characterization of SY-1365, a selective, covalent inhibitor of CDK7. *Cancer Res.* 79, 3479–3491.
- Huang, J.R., Qin, W.M., Wang, K., Fu, D.R., Zhang, W.J., Jiang, Q.W., Yang, Y., Yuan, M.L., Xing, Z.H., Wei, M.N., Li, Y., Shi, Z., 2018. Cyclin-dependent kinase 7 inhibitor THZ2 inhibits the growth of human gastric cancer in vitro and in vivo. *Am. J. Transl. Res.* 10, 3664–3676.
- Huang, T., Ding, X., Xu, G., Chen, G., Cao, Y., Peng, C., Shen, S., Lv, Y., Wang, L., Zou, X., 2019. CDK7 inhibitor THZ1 inhibits MCL1 synthesis and drives cholangiocarcinoma apoptosis in combination with BCL2/BCL-XL inhibitor ABT-263. *Cell Death Dis.* 10, 602.
- Labisso, W.L., Wirth, M., Stojanovic, N., Stauber, R.H., Schnieke, A., Schmid, R.M., Krämer, O.H., Saur, D., Schneider, G., 2012. MYC directs transcription of MCL1 and eIF4E genes to control sensitivity of gastric cancer cells toward HDAC inhibitors. *Cell Cycle* 11, 1593–1602.
- Larochelle, S., Merrick, K.A., Terret, M.E., Wohlbold, L., Barboza, N.M., Zhang, C., Shokat, K.M., Jallepalli, P.V., Fisher, R.P., 2007. Requirements for Cdk7 in the assembly of Cdk1/cyclin B and activation of Cdk2 revealed by chemical genetics in human cells. *Mol. Cell* 25, 839–850.
- Li, B., Ni Chonghaile, T., Fan, Y., Madden, S.F., Klinger, R., O'Connor, A.E., Walsh, L., O'Hurley, G., Mallya Udipi, G., Joseph, J., Tarrant, F., Conroy, E., Gaber, A., Chin, S.F., Bardwell, H.A., Provenzano, E., Crown, J., Dubois, T., Linn, S., Jirstrom, K., Caldas, C., O'Connor, D.P., Gallagher, W.M., 2017. Therapeutic rationale to target highly expressed CDK7 conferring poor outcomes in triple-negative breast cancer. *Cancer Res.* 77, 3834–3845.
- Liman, A., Shah, R., Passero, V., Tan, J., Rai, H., Harrold, L., Tokarsky, J., Liman, A., Gupta, V., Gerszten, K., 2020. The effect of radium-223 therapy in agent orange-related prostate carcinoma. *Fed. Pract.* 37, 570–574.
- Luo, H., Li, Q., O'Neal, J., Kreisel, F., Le Beau, M.M., Tomasson, M.H., 2005. c-Myc rapidly induces acute myeloid leukemia in mice without evidence of lymphoma-associated antiapoptotic mutations. *Blood* 106, 2452–2461.
- Malumbres, M., 2014. Cyclin-dependent kinases. *Genome Biol.* 15, 122.
- Medeiros, B.C., Satram-Hoang, S., Hurst, D., Hoang, K.Q., Momin, F., Reyes, C., 2015. Big data analysis of treatment patterns and outcomes among elderly acute myeloid leukemia patients in the United States. *Ann. Hematol.* 94, 1127–1138.
- Minzel, W., Venkatchalam, A., Fink, A., Hung, E., Brachya, G., Burstain, I., Shaham, M., Rivlin, A., Omer, I., Zinger, A., Elias, S., Winter, E., Erdman, P.E., Sullivan, R.W., Fung, L., Mercurio, F., Li, D., Vacca, J., Kaushansky, N., Shlush, L., Oren, M., Levine, R., Pikarsky, E., Snir-Alkalay, I., Ben-Neriah, Y., 2018. Small molecules co-targeting CK1 α and the transcriptional kinases CDK7/9 control AML in preclinical models. *Cell* 175, 171–185 e25.
- Mosley, A.L., Pattenden, S.G., Carey, M., Venkatesh, S., Gilmore, J.M., Florens, L., Workman, J.L., Washburn, M.P., 2009. Rtr1 is a CTD phosphatase that regulates RNA polymerase II during the transition from serine 5 to serine 2 phosphorylation. *Mol. Cell* 34, 168–178.
- Pan, X.N., Chen, J.J., Wang, L.X., Xiao, R.Z., Liu, L.L., Fang, Z.G., Liu, Q., Long, Z.J., Lin, D.J., 2014. Inhibition of c-Myc overcomes cytotoxic drug resistance in acute myeloid leukemia cells by promoting differentiation. *PLoS One* 9, e105381.
- Senichkin, V.V., Streletskaia, A.Y., Gorbunova, A.S., Zhivotovsky, B., Kopeina, G.S., 2020. Saga of Mcl-1: regulation from transcription to degradation. *Cell Death Differ.* 27, 405–419.
- Tibes, R., Bogenberger, J.M., 2019. Transcriptional silencing of MCL-1 through cyclin-dependent kinase inhibition in acute myeloid leukemia. *Front. Oncol.* 9, 1205.
- Veo, B., Danis, E., Pierce, A., Wang, D., Fosmire, S., Sullivan, K.D., Joshi, M., Khanal, S., Dahl, N., Karam, S., Serkova, N., Venkataraman, S., Vibhakhar, R., 2021. Transcriptional control of DNA repair networks by CDK7 regulates sensitivity to radiation in MYC-driven medulloblastoma. *Cell Rep.* 35, 109013.
- Wang, C., Jin, H., Gao, D., Wang, L., Evers, B., Xue, Z., Jin, G., Lieftink, C., Beijersbergen, R.L., Qin, W., Bernards, R., 2018. A CRISPR screen identifies CDK7 as a therapeutic target in hepatocellular carcinoma. *Cell Res.* 28, 690–692.
- Zhang, Y., Zhou, L., Bandyopadhyay, D., Sharma, K., Allen, A.J., Kmiecik, M., Grant, S., 2019. The covalent CDK7 inhibitor THZ1 potentially induces apoptosis in multiple myeloma cells in vitro and in vivo. *Clin. Cancer Res.* 25, 6195–6205.
- Zhong, S., Zhang, Y., Yin, X., Di, W., 2019. CDK7 inhibitor suppresses tumor progression through blocking the cell cycle at the G2/M phase and inhibiting transcriptional activity in cervical cancer. *OncoTargets Ther.* 12, 2137–2147.
- Zhou, Y., Lu, L., Jiang, G., Chen, Z., Li, J., An, P., Chen, L., Du, J., Wang, H., 2019. Targeting CDK7 increases the stability of Snail to promote the dissemination of colorectal cancer. *Cell Death Differ.* 26, 1442–1452.